Octahedral tilting evolution and phase transition in orthorhombic $NaMgF_3$ perovskite under pressure

H.-Z. Liu,[1,2] J. Chen,[3] J. Hu,[4] C. D. Martin,[3] D. J. Weidner,[3] D. Häusermann,[1] and H.-K. Mao[1,2]

Received 23 November 2004; revised 12 January 2005; accepted 21 January 2005; published 17 February 2005.

[1] Rietveld refinement of monochromatic synchrotron x-ray powder diffraction data was used to study the evolution of octahedral tilting in the orthorhombic $NaMgF_3$ perovskite under pressure. Hydrostatic pressure conditions were ensured up to 16 GPa using helium as a pressure medium. The tilting angles of MgF_6 octahedral framework were observed to increase with increasing pressure. The compression mechanism was observed to be dominated by the shortening of the octahedral Mg-F bond below 6 GPa, and then controlled by the increase of the octahedral tilting above 12 GPa. The bulk modulus of $NaMgF_3$ was estimated as 76.0 ± 1.1 GPa. A phase transition was observed at about 19.4 GPa in a separate run when silicone oil was used as pressure medium, and this high-pressure phase could be rationalized in term of a post-perovskite structural model. **Citation:** Liu, H.-Z., J. Chen, J. Hu, C. D. Martin, D. J. Weidner, D. Häusermann, and H.-K. Mao (2005), Octahedral tilting evolution and phase transition in orthorhombic $NaMgF_3$ perovskite under pressure, *Geophys. Res. Lett.*, *32*, L04304, doi:10.1029/2004GL022068.

[2] The driving force to low or high symmetry crystal structure in perovskite under pressure is of great interest due to the significant change in the physical properties during structural phase transitions. The fundamental understanding of the stable mechanisms of various perovskite structures upon compression has been a problem of long standing interest in condensed state physics, solid state chemistry, materials science and Earth science [*Ringwood*, 1962; *Glazer*, 1972; *Zhao*, 1998; *Kennedy et al.*, 2002]. Recently, a model [*Magyari-Köpe et al.*, 2002] which was based on the relative ionic overlaps and the global parametrization method, was presented on the octahedral rotation in orthorhombic perovskite structure. This model showed that hydrostatic pressure always stabilizes the less distorted structures in the universal bond picture of perovskite. However, in the real cases, this general trend is doubtable since the interaction between the semicore state of the cations and anions may be modulated by their individual bond character. For example, $MgSiO_3$ perovskite shows a very small increase in distortion as the pressure is increased [*Yagi et al.*, 1979]. In this report, $NaMgF_3$ perovskite (neighborite) was chosen to study the hydrostatic pressure effect on the tilting of its MgF_6 octahedra because neighborite has gained significant attention as an analogue of $MgSiO_3$ perovskite, which was believed to dominate in the Earth's lower mantle [*Ringwood*, 1962].

[3] Systematic studies of $NaMgF_3$ structure for its temperature-induced phase transition at room pressure as well as under high pressure conditions were performed by *Zhao et al.* [1993a, 1993b, 1994a, 1994b], following which *O'Keeffe and Bovin* [1979] *O'Keeffe et al.* [1979] pointed out the structural similarity between $NaMgF_3$ and $MgSiO_3$. A combined molecular dynamics simulations and neutron scattering study to investigate the thermal vibration on the average structure of $NaMgF_3$ was reported by *Street et al.* [1997]. Recently, the crystal chemistry of the potassium-bearing $(K_xNa_{1-x})MgF_3$ perovskite were studied by *Zhao* [1998] and *Chakhmouradian et al.* [2001]. However, no systematic structural refinement has been done for a sample maintained under hydrostatic high pressure conditions to study the pressure effect on the structure distortion from microstructure viewpoint. Most previous high pressure studies were carried out using energy dispersive x-ray diffraction (EDXRD) except one structural refinement for $NaMgF_3$ at 4.9 GPa based on monochromatic synchrotron x-ray diffraction [*Zhao et al.*, 1994b].

[4] The synthetic sample used in the present study was identical to that used in the previous studies [*Zhao et al.*, 1993a, 1993b, 1994a, 1994b], which was prepared by solid state reaction of NaF and MgF_2. The high pressure experiments were carried out in a diamond anvil cell (DAC) apparatus. The sample was loaded in a sample hole of T301 stainless steel gasket. Helium was used as pressure transmitting medium which can generate hydrostatic pressure conditions [*Takemura*, 2001]. The pressure was calibrated by the ruby luminescence method [*Mao et al.*, 1986]. The angle-dispersive X-ray diffraction (ADXRD) experiments (λ = 0.4028 Å) in a DAC were performed at room temperature at the beamline ID-B, HPCAT, Advanced Photon Source, Argonne National Laboratory. Diffraction patterns were recorded on a MAR345 image plate and then integrated by using the program FIT2D [*Hammersley et al.*, 1996].

[5] Figure 1 shows the typical XRD patterns of the sample under various pressures during the compressing process. No phase transition was observed within the experimental pressure range studied. The Rietveld refinements were carried out using the GSAS program package [*Larson and Von Dreele*, 1994] for all of the ADXRD patterns collected at hydrostatic pressure conditions. A

[1]High Pressure Collaborative Access Team, Advanced Photon Source, Argonne National Laboratory, Argonne, Illinois, USA.
[2]Also at Geophysical Laboratory, Carnegie Institution of Washington, Washington, D. C., USA.
[3]Mineral Physics Institute, State University of New York at Stony Brook, Stony Brook, New York, USA.
[4]Geophysical Laboratory, Carnegie Institution of Washington, Washington, D. C., USA.

0094-8276/05/2004GL022068$05.00

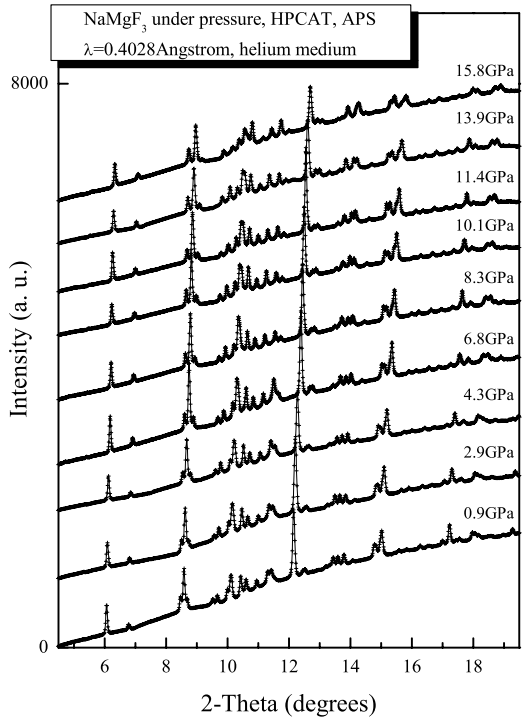

Figure 1. Typical ADXRD patterns of $NaMgF_3$ under hydrostatic pressure conditions during compression.

structural model at ambient conditions [*Zhao et al.*, 1994b] was used as a starting structure. Figure 2 shows the atomic displacements as a function of pressure, in which the fractional atomic coordinates of the *Pbnm* orthorhombic perovskite are defined with reference to a $Pm\bar{3}m$ cubic perovskite structure [*Zhao et al.*, 1993b].

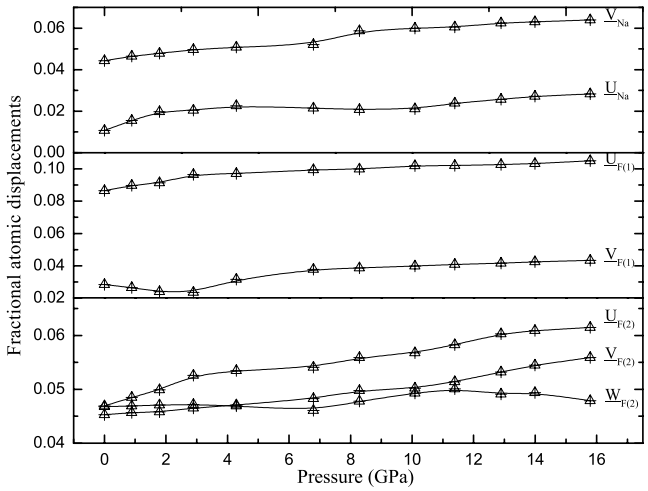

Figure 2. Fractional atomic displacements (referred to cubic $Pm\bar{3}m$ perovskite) of orthorhombic $NaMgF_3$ change as a function of pressure. Top: Na^+ cation moves straight along the *a*- and *b*-axis of the orthorhombic cell. Middle: The fractional displacements F(1) are related to the anti-phase tilting. Bottom: The displacements of F(2) are related to the in-phase tilting ($\underline{U}_{F(2)}$ and $\underline{V}_{F(2)}$) and anti-phase tilting ($\underline{W}_{F(2)}$). The lines are a guide to the eye.

[6] The lattice parameters of orthorhombic perovskite with space group *Pbnm* (Z = 4) could be expressed in terms of a pseudo-cubic prototype cell ($Pm\bar{3}m$, Z = 1). The previous heating experiments showed the continuous convergence of the pseudo-cubic lattice axes with increasing temperature at ambient condition [*Zhao et al.*, 1993a, 1993b], as well as under high pressure [*Zhao et al.*, 1994a], to a cubic structure. Figure 3 demonstrates the reduced unit cell parameters as a function of pressure. It is clear that the axes of the pseudo-cubic unit cell continuously diverge with increasing pressure, indicating pressure enhances the orthorhombic structural distortion. Thus, role of pressure on the structural distortion is opposite to that of temperature in $NaMgF_3$. This trend is in contrast to the general model that hydrostatic pressure always stabilizes the less distorted structures in perovskite [*Magyari-Köpe et al.*, 2002], but is in agreement with the compression behavior of $MgSiO_3$ [*Yagi et al.*, 1979].

[7] The centrosymmetrically distorted orthorhombic perovskite with space group *Pbnm* is distorted by two independent octahedral tilting θ and φ, where θ is an anti-phase tilt about the pseudo-cubic $\langle 110 \rangle_{pc}$ axes, and φ is an in-phase tilt about the pseudo-cubic $\langle 001 \rangle_{pc}$ axis of the octahedron. It can also be conceived as the tilting Φ about the threefold $\langle 111 \rangle_{pc}$ axes of the regular octahedra (see Figure 4 insertion for detail). The octahedral tilting of the $NaMgF_3$ perovskite could be quantitatively derived from the cell parameters (macro-approach) as well as from the positional parameters of atoms (micro-approach) [*Zhao et al.*, 1993a, 1993b]. Figure 4 shows the octahedral tilting as a function of pressure from both macro and micro methods. The overall trends of the octahedral tilting angles, i.e., increasing with increasing pressure, are similar for both macro and micro approaches. The tilting angles which are derived from lattice parameters are underestimated due to the assumed regularity of the octahedron. It is noticed that the derivation of the octahedral titling angles from unit cell

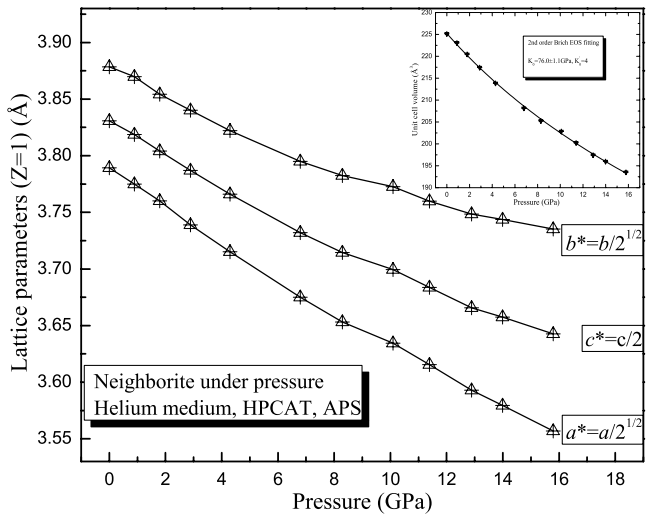

Figure 3. Unit cell parameters (reduced to a pseudo-cubic Z = 1 subcell) of $NaMgF_3$ perovskite as a function of pressure. The lines are a guide to the eye. Insertion shows the volume compression data and the fitting according to second-order Birch EOS.

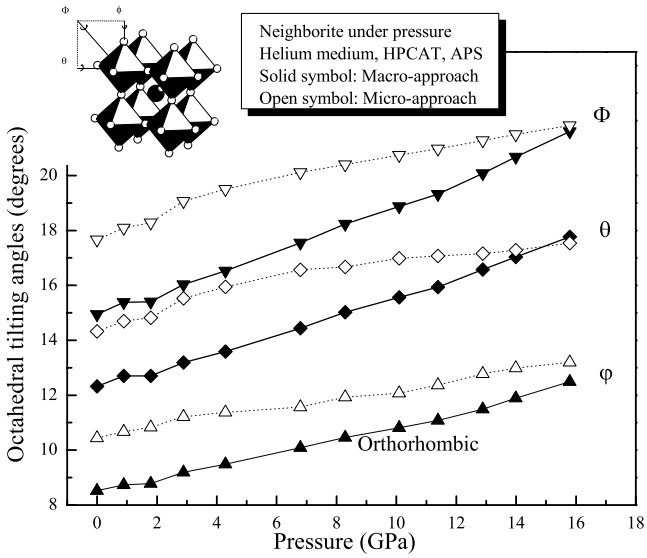

Figure 4. Pressure evolution of the octahedral tilting angles of $NaMgF_3$ perovskite as derived from lattice parameters (macro-approach), and atomic positions (micro-approach) plotted as solid and open symbols, respectively. Insertion shows the octahedral tilting angles referred to an ideal cubic $Pm\bar{3}m$ perovskite. See color version of this figure in the HTML.

parameters and atomic positions are only accurate when the assumption of rigid octahedra is valid, and the octahedral tilting angles are small [*Zhao et al.*, 1993a, 1993b]. Since pressure enhances the structural distortion in this orthorhombic perovskite case, these assumptions do not remain valid any more. The octahedral tilting angles derived from lattice parameters or from atomic positions under high pressure, basically provide the relative values of the octahedral tilting angles.

[8] The lattice distortion and thus the ferroelastic feature are the direct results introduced by octahedral tilting. The spontaneous strain is applied to characterize these and its magnitude for this ferroic species of *m*3*mFmmm* can be expressed as a function of lattice parameters [*Zhao et al.*, 1993b]. Figure 5 illustrates the spontaneous strain as a function of pressure. It increases continuously with increasing pressure. Previous results are also plotted for comparison. The overestimation of the spontaneous strain in the large volume cell (LVC) energy dispersive XRD (EDXRD) data [*Zhao et al.*, 1994a] may partly be due to its relative non-hydrostatic conditions. In addition the relative inaccuracy of lattice parameters derived from EDXRD data could also be a cause. The ADXRD high pressure LVC experiment [*Zhao et al.*, 1994b] at 4.9 GPa had been carefully annealed under pressure to release deviatoric stresses. We believed that this is corroborated by this result in good agreement with our results in Figure 5.

[9] The contribution of octahedral tilting and the octahedral bond length to the volumetric compression could be decoupled as [*Zhao et al.*, 1993a, 1994a, 1994b]:

$$\beta_V = \beta_{V0} + \beta_{V_\Phi} = \frac{-3\partial[Mg-F]}{[Mg-F]\partial P} + \frac{-2\partial\cos\Phi}{\cos\Phi\partial P}$$

This compression mechanism was analyzed in previous high pressure studies, and the compression of octahedral bond length was found to contribute about 70–80% to the overall volumetric compression within about 5 GPa [*Zhao et al.*, 1994a, 1994b]. In this report, the contribution to the volumetric compression from octahedral bond length and tilting were estimated from the unit cell parameters, and Figure 6 illustrates β_V, β_{V0}, and $\beta_{V\Phi}$ change as a function of pressure. It is shown that volumetric compression was dominated by the shortening of the octahedral Mg-F bond at beginning of compression below 6 GPa. Between 6–12 GPa

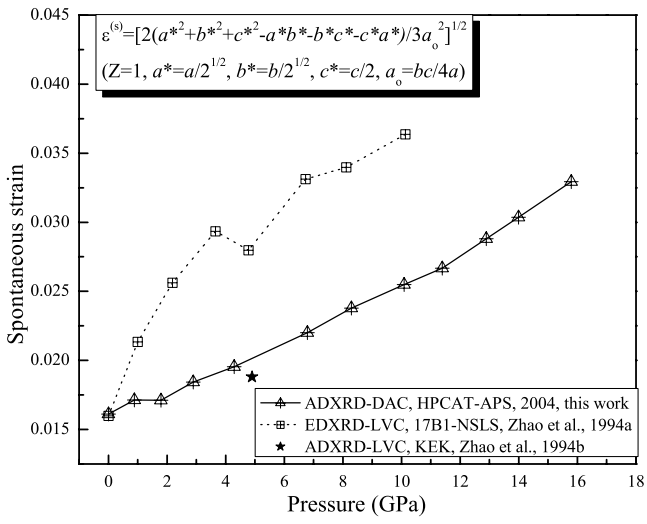

Figure 5. The spontaneous strain of $NaMgF_3$ perovskite as a function of pressure.

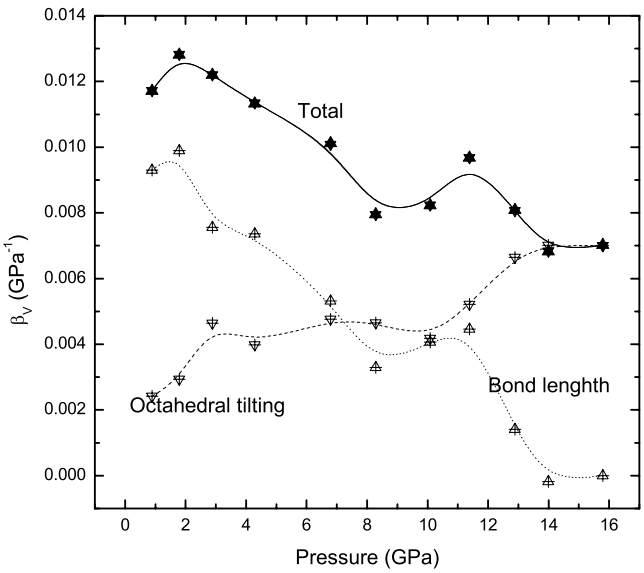

Figure 6. Total volumetric compression β_V, and the octahedral tilting $\beta_{V\Phi}$ and the octahedral bond length β_{V0} contribution to volumetric compression as a function of pressure.

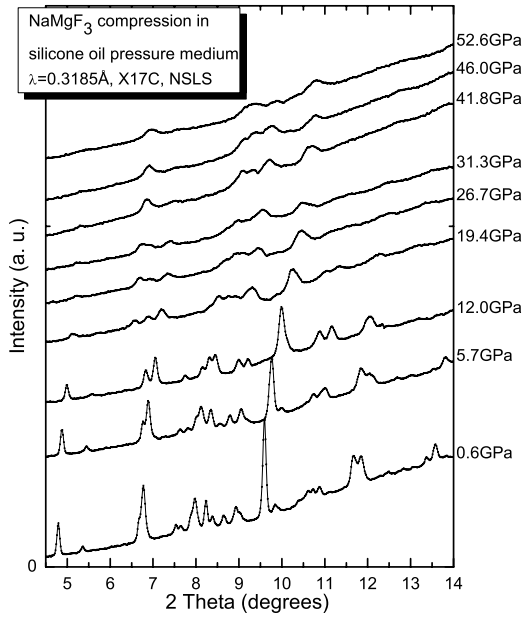

Figure 7. Typical ADXRD patterns of $NaMgF_3$ during compression when silicone oil was used as a pressure medium.

pressure range, the contribution from the octahedral tilting matches that of bond length compression. This is following by an increasing contribution from the octahedral tilting above 12 GPa. Since the decoupled volumetric compression mechanism is based on the assumption that octahedra remain regular under compression, this model should not work well at higher pressures where the pressure induced structural distortion increases and in turn made the MgF_6 octahedra gradually lose their regularity.

[10] The equation of state of $NaMgF_3$ could be fitted using a second-order Birch equation of state (EOS) (shown as insertion in Figure 3), keeping the pressure derivative of bulk modulus K'_0 as 4 [*Birch*, 1978]. The zero pressure bulk modulus (K_0) is estimated as 76.0 ± 1.1 GPa, which is in good agreement with the bulk modulus value of 75.6 GPa measured from single crystal Brillouin scattering [*Zhao and Weidner*, 1993].

[11] The octahedral tilting increasing with pressure finally destroys the perovskite structure. A separate experiment was carried out using silicone oil as pressure medium which could generate more shear stress to accelerate the phase transition, and performed at X17C, National Synchrotron Light Source (NSLS). Figure 7 shows the selected XRD patterns during compression. It demonstrates a phase transition at about 19.4 GPa, and the patterns above this pressure can no longer be indexed by the *Pbnm* perovskite structure, but can be indexed with the layering-type post-perovskite structural model [*Murakami et al.*, 2004; *Iitaka et al.*, 2004; *Oganov and Ono*, 2004; *Shim et al.*, 2004; *Mao et al.*, 2004] with space group *Cmcm*. A cell with lattice parameters a = 2.780 Å, b = 8.491 Å, and c = 7.001 Å could index the XRD pattern at 31.3 GPa in Figure 7. This new phase is quenchable, and is stable at ambient conditions for at least 2 days. This encouraged us to perform further studies in this quenchable sample in the near future. We intend to study the elastic and other physical properties of this post-perovskite phase.

[12] **Note added in Proof.** Two independent theoretical calculations [*Parise et al.*, 2004; A. R. Oganov, unpublished data, 2005] confirmed this pressure induced phase transition in neighborite.

[13] **Acknowledgments.** HPCAT facility was supported by DOE-BES, DOE-NNSA (CDAC), NSF, DOD-TACOM, and W. M. Keck Foundation. This work was partially supported by COMPRES. H. L. thanks M. Somayazulu for helpful discussions.

References

Birch, F. (1978), Finite strain isotherm and velocities for single-crystal and polycrystalline NaCl at high pressures and 300 K, *J. Geophys. Res.*, *83*, 1257–1269.

Chakhmouradian, A. R., K. Ross, R. H. Mitchell, and I. Swainson (2001), The crystal chemistry of synthetic potassium-bearing neighborite, $(Na_{1-x}K_x)MgF_3$, *Phys. Chem. Miner.*, *28*, 277–284.

Glazer, A. M. (1972), The classification of tilted octahedra in perovskites, *Acta Crystallogr., Sect. B Struct. Sci.*, *28*, 3384–3392.

Hammersley, A. P., S. O. Svensson, M. Hanfland, A. N. Fitch, and D. Häusermann (1996), Two-dimensional detector software: From real detector to idealised image or two-theta scan, *High Pressure Res.*, *14*, 235–248.

Iitaka, T., K. Hirose, K. Kawamura, and M. Murakami (2004), The elasticity of $MgSiO_3$ post-perovskite phase in the Earth's lowermost mantle, *Nature*, *430*, 442–445.

Kennedy, B. J., T. Vogt, C. D. Martin, J. B. Parise, and J. A. Hriljac (2002), Pressure-induced phase transition in $PrAlO_3$, *Chem. Mater.*, *14*, 2644–2648.

Larson, A. C., and R. B. Von Dreele (1994), General Structure Analysis System (GSAS), *Los Alamos Natl. Lab. Rep. LAUR 86–748*, Los Alamos, N. M.

Magyari-Köpe, B., L. Vitos, B. Johansson, and J. Kollár (2002), Origin of octahedral tilting in orthorhombic perovskite, *Phys. Rev. B*, *66*, doi:10.1103/PhysRevB.66.092103.

Mao, H. K., J. Xu, and P. M. Bell (1986), Calibration of the ruby pressure gauge to 800-kbar under quasi-hydrostatic conditions, *J. Geophys. Res.*, *91*, 4673–4676.

Mao, W. L., G. Shen, V. B. Prakapenka, Y. Meng, A. J. Campbell, D. L. Heinz, J. Shu, R. J. Hemley, and H. K. Mao (2004), Ferromagnesian postperovskite silicates in the D″ layer of the Earth, *Proc. Natl. Acad. Sci. U. S. A.*, *101*, 15,867–15,869.

Murakami, M., K. Hirose, K. Kawamura, N. Sata, and Y. Ohishi (2004), Post-perovskite phase transition in $MgSiO_3$, *Science*, *304*, 855–858.

Oganov, A. R., and S. Ono (2004), Theoretical and experimental evidence for a post-perovskite phase of $MgSiO_3$ in Earth's D″ layer, *Nature*, *430*, 445–448.

O'Keeffe, M., and J. O. Bovin (1979), Solid electrolyte behavior of $NaMgF_3$: Geophysical implications, *Science*, *206*, 599–600.

O'Keeffe, M., B. G. Hyde, and J. O. Bovin (1979), Contribution to the crystal chemistry of orthorhombic perovskite: $MgSiO_3$ and $NaMgF_3$, *Phys. Chem. Miner.*, *4*, 299–305.

Parise, J., K. Umemoto, R. M. Wentzcovitch, and D. Weidner (2004), Post-perovskite transition in $NaMgF_3$, *Eos Trans. AGU*, *85*(47), Fall Meet. Suppl., Abstract MR23A-0188.

Ringwood, A. E. (1962), Mineralogical constitution of the deep mantle, *J. Geophys. Res.*, *67*, 4005–4010.

Shim, S., T. S. Duffy, R. Jeanloz, and G. Shen (2004), Stability and crystal structure of perovskite to the core-mantle boundary, *Geophys. Res. Lett.*, *31*, L10603, doi:10.1029/2004GL019639.

Street, J. N., I. G. Wood, K. S. Knight, and G. D. Price (1997), The influence of thermal vibrations on the average structure of cubic $NaMgF_3$ perovskite: A combined molecular dynamics and neutron diffraction study, *J. Phys. Condens. Matter*, *9*, L647–L655.

Takemura, K. (2001), Evaluation of the hydrostaticity of a helium-pressure medium with powder x-ray diffraction techniques, *J. Appl. Phys.*, *89*, 662–668.

Yagi, T., H. K. Mao, and P. M. Bell (1979), Hydrostatic compression of $MgSiO_3$ of perovskite structure, *Year Book Carnegie Inst. Washington*, *78*, 613–614.

Zhao, Y. S. (1998), Crystal chemistry and phase transitions of perovskite in P-T-X space: Data for $(K_xNa_{1-x})MgF_3$ perovskites, *J. Solid State Chem.*, *141*, 121–132.

Zhao, Y. S., and D. J. Weidner (1993), The single crystal elastic moduli of neighborite, *Phys. Chem. Miner.*, *20*, 419–424.

Zhao, Y. S., D. J. Weidner, J. B. Parise, and D. E. Cox (1993a), Thermal expansion and structural distortion of perovskite—Data for $NaMgF_3$ perovskite. Part I, *Phys. Earth Planet. Inter.*, *76*, 1–16.

Zhao, Y. S., D. J. Weidner, J. B. Parise, and D. E. Cox (1993b), Critical phenomena and phase transition of perovskite—Data for $NaMgF_3$ perovskite. Part II, *Phys. Earth Planet. Inter.*, *76*, 17–34.

Zhao, Y. S., et al. (1994a), Perovskite at high P-T conditions: An in situ synchrotron X ray diffraction study of $NaMgF_3$ perovskite, *J. Geophys. Res.*, *99*, 2871–2885.

Zhao, Y. S., J. B. Parise, Y. B. Wang, K. Kusaba, M. T. Vaughan, D. J. Weidner, T. Kikegawa, J. H. Chen, and O. Shimomura (1994b), High-pressure crystal chemistry of neighborite, $NaMgF_3$: An angle-dispersive diffraction study using monochromatic synchrotron X-radiation, *Am. Mineral.*, *79*, 615–621.

D. Häusermann, H.-Z. Liu, and H.-K. Mao, High Pressure Collaborative Access Team, Advanced Photon Source, Argonne National Laboratory, Argonne, IL 60439, USA. (hliu@hpcat.aps.anl.gov)

J. Hu, Geophysical Laboratory, Carnegie Institution of Washington, 5251 Broad Branch Rd., N.W, Washington, DC 20015, USA.

J. Chen, C. D. Martin, and D. J. Weidner, Mineral Physics Institute, State University of New York at Stony Brook, Stony Brook, NY 11794–2100, USA.